

This discussion paper is/has been under review for the journal *Atmospheric Chemistry and Physics (ACP)*. Please refer to the corresponding final paper in *ACP* if available.

Hygroscopic growth of urban aerosol particles in Beijing

J. Meier et al.

Hygroscopic growth of urban aerosol particles in Beijing (China) during wintertime: a comparison of three experimental methods

J. Meier¹, B. Wehner¹, A. Massling^{1,*}, W. Birmili¹, A. Nowak¹, T. Gnauk¹, E. Brüggemann¹, H. Herrmann¹, H. Min², and A. Wiedensohler¹

¹Leibniz Institute for Tropospheric Research, Leipzig, Germany

²College of Environmental Sciences, Peking University, Beijing, China

*now at: National Environmental Research Institute, Roskilde, Denmark

Received: 30 January 2009 – Accepted: 10 February 2009 – Published: 16 March 2009

Correspondence to: J. Meier (jessica.meier@tropos.de)

Published by Copernicus Publications on behalf of the European Geosciences Union.

Title Page

Abstract

Introduction

Conclusions

References

Tables

Figures

◀

▶

◀

▶

Back

Close

Full Screen / Esc

Printer-friendly Version

Interactive Discussion



Abstract

This paper presents hygroscopicity measurements of aerosol particles in the urban atmosphere of Beijing carried out in January 2005. Therefore, three different methods were used: 1) Combining Humidifying Differential Mobility Particle Sizer (H-DMPS) and Twin Differential Mobility Particle Sizer (TDMPS) measurements; 2) Hygroscopicity Tandem Differential Mobility Analyzer (H-TDMA) technique; 3) Calculating hygroscopic growth factors on the basis of a solubility model quantified by Micro Orifice Uniform Deposit Impactor (MOUDI) samples. Particle number size distributions from H-DMPS and TDMPS were evaluated to derive size-resolved descriptive hygroscopic growth factors (DHGF) of 30–400 nm particles at relative humidities (RH) of 55%, 77% and 90%. The atmospheric particles in Beijing were rather hydrophobic, with a maximum growth factor in the accumulation mode around 1.40 (± 0.03) at 90% RH. The descriptive hygroscopic growth factors decreased significantly towards the lower measurement limit (1.04 (± 0.15) at $D_p=30$ nm). A good agreement was found between the DHGFs and the H-TDMA-derived hygroscopic growth factors in the accumulation mode (100–400 nm), the DHGFs underestimated the values from the H-TDMA in the Aitken mode (<100 nm) by up to 0.1 at 90% RH. The calculation of hygroscopic growth factors based on the measured chemical composition showed that different modes of combining the inorganic ions caused a variation in growth factor of 0.1 at 90% RH. The solubility model was able to reproduce the size-dependent trend in the growth factor found by the other methods. In two cases of ion-dominated aerosol, the composition-derived growth factors tended to agree (± 0.05) or underestimate (up to 0.1) the values measured by the other two methods. In the case of the organic-dominated aerosol, the reverse was true, with an overestimation of up to 0.2. The results shed light on the real experimental and methodological uncertainties that are still connected with the determination of hygroscopic growth factors.

ACPD

9, 6889–6927, 2009

Hygroscopic growth of urban aerosol particles in Beijing

J. Meier et al.

Title Page

Abstract

Introduction

Conclusions

References

Tables

Figures

◀

▶

◀

▶

Back

Close

Full Screen / Esc

Printer-friendly Version

Interactive Discussion



1 Introduction

Beijing is one of the large industrial centres in China, with a population of about 15 million only within its administrative district. The present Beijing has been shaped by the enormous economic growth that occurred during the last two decades (Tang et al., 2005). This growth has brought about an enormous increase of energy consumption, mainly from fossil fuels like coal and natural gas. During winter domestic heating accounts for a great deal of the energy consumption, whereas in summer air conditioning requires large amounts of additional electrical power. Although China has undertaken major efforts towards exploiting renewable energy sources such as hydroelectric power and cleaner combustion methods such as coal briquettes, the combustion of fossil fuels will remain the mainstay of the Chinese energy supply in the foreseeable future.

The combustion of fossil fuels have led to environmental problems associated with the pollution gases and particles emitted into the atmosphere. In contrast to Europe and the US, sulphur is still ubiquitous in fuel in China. Particle pollution has led to the prevalence of lung and heart diseases, with the total mortality suggested to increase by 11% with each doubling of the sulphur dioxide concentration (Xu et al., 1994). Indoor air quality is widely degraded by the use of unvented stoves fuelled by coal or biomass (Florig, 1997). The industrial raise in China has led to air pollution that has been acknowledged to greatly influences regional climate, and influence the worldwide level of air pollutants as well (Mage et al., 1996; Fenger, 1999).

Measurements of atmospheric particles in China have been intensified during the last decade, with the aim of better defining particle mass and size distribution, as well as chemical composition and optical properties. Bergin et al. (2001) observed that in Beijing, the single scattering albedo and the daily mean value for the $PM_{2.5}$ mass concentration were considerably higher than, for instance, in the US industrial regions. Bergin et al. (2001) suggested that the poor visibility may be due mainly to locally and regionally combustion particles. Over Beijing, the winter-time atmospheric optical depth increased by a factor of about two over the past 15 years, with the increasing

Hygroscopic growth of urban aerosol particles in Beijing

J. Meier et al.

Title Page

Abstract

Introduction

Conclusions

References

Tables

Figures



Back

Close

Full Screen / Esc

Printer-friendly Version

Interactive Discussion



local and regional energy production being a prime reason. In summer time, the optical depths may, however, be even larger because of the higher relative humidity and the associated hygroscopic particle growth (Jinhuan and Liqun, 2000). It is worth to note that natural aerosols play a role for the local air quality as well: visibilities of less than 1 km may be caused during dust storm events (Zhang et al., 2003; Sugimoto et al., 2003).

With the aid of long-term observations of particle number size distributions, specific atmospheric aerosol types and their particular relevance for the air quality in Beijing could be identified: coarse mineral particles resulting from dust storms in inner Asia (Wehner et al., 2004), direct emissions from primary sources as well as secondary aerosol formation in the Aitken and accumulation mode (Wu et al., 2007), and ultrafine particles (diameter <40 nm) formed on a regional scale especially in air masses from inner Asia (Wehner et al., 2008). The latter work also highlighted the importance of slowly moving air masses under high pressure influence, which causes the highest overall levels of particulate pollution in Beijing.

The hygroscopic growth of aerosol particles along with relative humidity greatly influences their backscattering of solar radiation (Charlson and Heintzenberg, 1995) and thus, atmospheric visibility (Tang et al., 1981). Most atmospheric aerosols are externally mixed with respect to hygroscopicity, and consist of more and less hygroscopic sub-fractions (Swietlicki et al., 2008). The ratio between these fractions as well as the fraction of soluble material determines the hygroscopic growth of the overall aerosol. The ability of ambient aerosol to take up water may vary from day to day, from place to place, and with particle size (McMurry and Stolzenburg, 1989; Cocker et al., 2001; Swietlicki et al., 2008), although to a much lesser extent than total particle mass and number. Generally, the fraction of hydrophobic particles increases with proximity to urban sources (Ferron et al., 2005). The hygroscopic behavior of urban aerosols was characterised as a mostly trimodal mixture (nearly hydrophobic, less hygroscopic and more hygroscopic), whose relative number depended on the time of day, day of the week, and season (Massling et al., 2005).

Hygroscopic growth of urban aerosol particles in Beijing

J. Meier et al.

Title Page

Abstract

Introduction

Conclusions

References

Tables

Figures

◀

▶

◀

▶

Back

Close

Full Screen / Esc

Printer-friendly Version

Interactive Discussion



**Hygroscopic growth
of urban aerosol
particles in Beijing**J. Meier et al.

For China, only three experimental studies on the hygroscopic growth of tropospheric aerosol particles have been reported to the date of writing. Eichler et al. (2008) reported hygroscopic growth factors of the aerosol over the south Chinese Pearl River Delta, whose influence on the associated optical properties were subsequently discussed by Cheng et al. (2008). Measurements during the Carebeijing-2006 project served to characterise the hygroscopic properties of regional aerosols over the North China Plain (i.e. about 50 km south of Beijing) during summertime (Achtert et al., 2009). The urban aerosol in Beijing itself has been characterised during two field campaigns and winter: Massling et al. (2009) suggest that the hygroscopic growth factors of Aitken and accumulation mode particles were slightly lower than comparable European observations, but nevertheless dominated by sulfate as main soluble component.

In January 2005, a specialised field campaign was conducted to further characterise the hygroscopic growth of sub-micrometer aerosol particles in the urban atmosphere of Beijing. Hygroscopic particle growth is instrumental in describing the ambient particle size distribution, and its associated aerosol dynamical and optical effects such as visibility and single scattering albedo. As a novelty, three different experimental techniques were used to determine hygroscopic growth factors. These are either based on particle mobility spectrometers (TDMPS/H-DMPS, H-TDMA), or on the combination of chemical composition measurements with a solubility model. This paper discusses the comparison between the methods as well as the overall results as a function of the local weather during the observation period. Tables are provided to make the measurement data accessible for further calculations related to the effects of the ambient aerosol in Beijing.

[Title Page](#)[Abstract](#)[Introduction](#)[Conclusions](#)[References](#)[Tables](#)[Figures](#)[⏪](#)[⏩](#)[◀](#)[▶](#)[Back](#)[Close](#)[Full Screen / Esc](#)[Printer-friendly Version](#)[Interactive Discussion](#)

2 Experimental

2.1 Measurement campaign in Beijing

Intensive atmospheric aerosol measurements were carried out in Beijing (39.9° N, 116.4° E), China, between 17 and 25 January 2005. The Chinese capital is situated within the North Chinese Lowlands, about 110 km north-west of the Golf of Bo Hai. All measurements were performed on the campus of the University of Beijing located between the fourth and fifth circular road in the northern part of the city. The container for the in-situ measurements was placed between a faculty building and a quiet, small street with very rare vehicle traffic. The overall vehicle traffic on the campus is not very dense, and is assumed to play a minor role only. Further contributions to the measurements may originate from domestic heating and cooking activities within the campus as well as the motor traffic outside. Freight trucks are permitted to enter the city centre only during nighttime. For this reason, Beijing is exposed to traffic particulate emissions all the time: passenger and light-duty traffic during daytime, and heavy supply traffic during nighttime. Additional emissions during our observational period arose from domestic heating. Furthermore, the air pollution in the city may strongly be influenced by pollution from highly populated North China Plain south of Beijing during certain periods. Beijing's climate can be termed moderate continental: hot and humid summers are followed by cold and dry winters. During our measurements low ambient temperatures (−6.6–4.9°C, average: −1.1°C) and relative humidities (14–71%, average: 38%) prevailed.

Our aerosol particle measurements included a Twin Differential Mobility Particle Sizer (TDMPS), a Humidifying-Differential Mobility Particle Sizer (H-DMPS), a Hygroscopicity-Tandem Differential Mobility Analyzer (H-TDMA), and chemical particle analysis of samples collected using a Micro Orifice Uniform Deposit Impactor (MOUDI). The TDMPS and H-DMPS instruments were placed inside an air-conditioned measurement container. Both systems were supplied with aerosol that had passed through a PM₁₀ impaction inlet mounted 2.3 m above the container roof. The MOUDI and the

Hygroscopic growth of urban aerosol particles in Beijing

J. Meier et al.

Title Page

Abstract

Introduction

Conclusions

References

Tables

Figures

◀

▶

◀

▶

Back

Close

Full Screen / Esc

Printer-friendly Version

Interactive Discussion



H-TDMA were placed inside an air-conditioned laboratory on the top (20 m height) of a nearby building, distant at 200 m.

2.2 Twin Differential Mobility Particle Sizer

A Twin Differential Mobility Particle Sizer (TDMPS) was used to measure dry number size distributions of ambient particles (3–900 nm). Atmospheric particles were dried to a relative humidity (RH) below 20% in a diffusion dryer upstream of the instrument. Sheath air was supplied at a relative humidity below 5% for the Differential Mobility Analyzers (DMAs). The TDMPS consists of two DMA subsystems covering size ranges of 3–22 nm and 22–900 nm, respectively (Birmili et al., 1999). The data reduction scheme includes a multiple charge inversion (Stratmann and Wiedensohler, 1996) that accounts for the DMA transfer functions, and the counting efficiencies of the condensation particle counters. As a last step, the losses of particles due to diffusion in the inlet system were corrected by using analytical formula for laminar flow.

2.3 The Humidifying DMPS

The Humidifying DMPS (H-DMPS) is a recently built-up variant of the DMPS that measures particle number size distributions at controlled relative humidity (Eichler et al., 2008; Birmili et al., 2009). Briefly, the H-DMPS consists of a single DMA measuring particles across the diameter range 22–900 nm. Particles are first humidified to above 90% RH upstream of the DMA, and subsequently dried down to target RH. This ensures that the particles are in a state above the deliquescence point. The sample aerosol is conditioned to the target RH of either 55%, 77% or 90% before entering the bipolar charger and the DMA. Sheath air is supplied to the DMA at the same RH. Small fluctuations in room temperature may lead to erroneous RHs during particle classification. Therefore, a careful quality control of the H-DMPS size distributions were needed with RH in the DMA excess flow being used as the main quality control parameter. A detailed account on the quality control of the H-DMPS data is given in Birmili et al.

Hygroscopic growth of urban aerosol particles in Beijing

J. Meier et al.

Title Page

Abstract

Introduction

Conclusions

References

Tables

Figures

◀

▶

◀

▶

Back

Close

Full Screen / Esc

Printer-friendly Version

Interactive Discussion



(2009).

2.4 The Hygroscopic Tandem DMA

The H-TDMA instrument used in this study is based on the set-up originally described by Rader and McMurry (1986). It consists of two DMAs and an aerosol humidifier, which is positioned between the DMAs. The first DMA selects a monodisperse fraction of particles at dry conditions. These particles with defined particle sizes (here $D_p=30, 50, 80, 150, 250$ and 350 nm) pass through a humidifier to be conditioned to defined RH (here: 90%). The second DMA was operated with a sheath air of 90% RH and coupled to a condensation particle counter to measure the number size distribution of the humidified altered aerosol. The measured number size distribution provides a hygroscopic growth factor spectrum depending on the state of mixing. More details of the instrument can be found in Massling et al. (2005).

2.5 Chemical particle sampling and analysis

Bulk particles were collected across an ambient aerodynamic diameter range $0.056\text{--}18$ μm by a Micro Orifice Uniform Deposit Impactor (MOUDI; Marple et al., 1991). After transport to the laboratory, the samples were analysed for the carbonaceous component as well as inorganic ions. Before and after exposure the impactor foils were equilibrated for 48 hours at constant temperature ($20\pm 2^\circ\text{C}$) and relative humidity ($50\pm 5\%$). The foils were weighed by a microbalance UMT-2 (Mettler-Toledo, Giessen, Germany) with a reading precision of 0.1 μg and a standard deviation of ≤ 1 μg . The absolute particle mass varied from 5 μg ($D_{\text{aero}}=0.056\text{--}0.1$ μm) to 3500 μg ($D_{\text{aero}}=0.32\text{--}0.56$ μm) corresponding to a relative error of 20 to 0.03%. In the range of 100 μg weighed mass, the relative error is in the range of 1%.

Cations were determined by ion chromatography (IC-Metrohm AG, Herisau, Switzerland), anions by capillary zone electrophoresis (CE-Spectra Phoresis 1000, Thermo Separation Products, USA). A detailed description is given by Brüggemann and Rolle

Hygroscopic growth of urban aerosol particles in Beijing

J. Meier et al.

Title Page

Abstract

Introduction

Conclusions

References

Tables

Figures

◀

▶

◀

▶

Back

Close

Full Screen / Esc

Printer-friendly Version

Interactive Discussion



(1998) and Neusüss et al. (2000). Particulate carbon determination was performed with a thermographic method similar to the VDI-guideline (VDI 2465, Part 2) in Germany using a carbon analyzer C-mat 5500 (Ströhlein, Viersen, Germany). The aluminium foil aliquot was in a first step heated to 650°C under nitrogen atmosphere for eight minutes. Those carbon compounds that evaporate under these conditions are referred to as organic carbon (OC). Evaporated OC is oxidised quantitatively on a CuO-catalyst at 850°C to CO₂ and measured in a NDIR detector. In a second step, the remaining elemental carbon (EC) was determined by burning the sample under oxygen atmosphere at 650°C for eight minutes, whereby all carbon is oxidised to CO₂ and then detected also by IR absorption. Further details of the carbon analysis are described in Neusüss et al. (2000).

3 Calculation of hygroscopic growth factors

The basic definition of the hygroscopic growth factor calculation is the quotient between the particle diameter as measured at a certain relative (reference) humidity RH₁, and the diameter measured at a second humidity RH₂, with RH₁ being usually higher than RH₂.

$$GF = \frac{D_p(RH_1)}{D_p(RH_2)} \quad (1)$$

The three methodologies to determine hygroscopic growth factors are outlined in the following.

3.1 Descriptive hygroscopic growth factors from TDMPS and H-DMPS

In the field, the H-DMPS and TDMPS measurements were triggered and thus available for corresponding 10 min intervals. Descriptive hygroscopic growth factors were calculated from paired dry/humidified distributions using the summation method (SM).

Hygroscopic growth of urban aerosol particles in Beijing

J. Meier et al.

Title Page

Abstract

Introduction

Conclusions

References

Tables

Figures

◀

▶

◀

▶

Back

Close

Full Screen / Esc

Printer-friendly Version

Interactive Discussion



Hygroscopic growth of urban aerosol particles in Beijing

J. Meier et al.

Title Page

Abstract

Introduction

Conclusions

References

Tables

Figures

◀

▶

◀

▶

Back

Close

Full Screen / Esc

Printer-friendly Version

Interactive Discussion



As the SM derives growth factors averaging over all hygroscopic particle fractions, its output function was termed “Descriptive Hygroscopic Growth Factor” (DHGF). The SM allocates segments of equal particle number under the dry and humidified (here: 55%, 77% and 90% RH) number size distributions, starting at the upper tail of the number size distribution, and moving downwards. It is assumed that the particles in the “dry” number segment grow, on average, to the corresponding “wet” number segment. The DHGF is the diameter ratio of the mean diameters of both segments. For further details of the calculation method we refer to the description in Birmili et al. (2009).

We are aware that the assumption of homogeneously mixed particles is not true in atmospheric aerosols, since they tend to be externally mixed (Swietlicki et al., 2008). However, the procedure is assumed to yield trustworthy results as long as no dramatic changes occur in terms of the external particle mixture with particle diameter. The DHGF represents, in fact, a hygroscopic growth factor averaged for the dry monodisperse population rather than the individual growth factors of less and more hygroscopic particle fractions. The upper size limit of the SM is limited by the counting statistics in the upper accumulation mode range, whereas its lower size limit is defined by the degree of absolute comparability between TDMPs and H-DMPS size distributions. Taking both issues into account, the range of DHGFs is limited to 30–500 nm.

3.2 Growth factors from H-TDMA

In this study atmospheric particles were separated into groups with different hygroscopic growth named “nearly hydrophobic”, “less hygroscopic” and “more hygroscopic” (Massling et al., 2003). According to this classification three growth factors (GF_1 , GF_2 , GF_3) and their corresponding number fractions (nf_1 , nf_2 , nf_3) were obtained in dependence of investigated dry diameter. To compare these results with the DHGF of the H-DMPS/TDMPs measurements a mean \overline{GF} was calculated by

$$\overline{GF} = \sqrt[3]{nf_1 \cdot GF_1^3 + nf_2 \cdot GF_2^3 + nf_3 \cdot GF_3^3} \quad (2)$$

3.3 Growth factors from chemical composition

The analysis of the particle chemical composition was restricted to soluble ions such as Na^+ , NH_4^+ , K^+ , Ca^{2+} , Mg^{2+} , Cl^- , SO_4^{2-} and NO_3^- and the insoluble material here was assigned to as elemental carbon (EC) and organic carbon (OC).

Based on the real mass (individual components) of each impactor stage sample, the hygroscopic diameter growth factors of MOUDI samples were calculated. Therefore, the mass of organic carbon (OC) was converted into the mass of organic matter (OM) by means of a factor of 1.6 (urban aerosol) to account for the non-carbon material (Turpin and Lim, 2001).

The calculated hygroscopic growth factors (CHGFs) were carried out based on the obtained mass of ions. The masses were converted into amount of substance and using these values, the amount of possible compounds, i.e. salts, was determined. These obtained salts (in this case: NaCl , NaNO_3 , NH_4NO_3 and $(\text{NH}_4)_2\text{SO}_4$) were assumed to represent the main compounds of the atmospheric aerosol sample observed during the three measurement time periods of the MOUDI (I1, I2, I3 as defined later). Additionally, it was assumed that freshly formed sulfuric acid (H_2SO_4) was also a compound of the observed aerosol, when SO_4^{2-} -ions were not neutralised by the present positive ions. Because of the correlation between NH_4^+ and $[\text{SO}_4^{2-} + \text{NO}_3^-]$ (I1: $R=0.97$; I2: $R=0.98$; I3: $R=0.97$) these components were used to form the corresponding salts. NaCl was assumed to be one of the main compounds of the atmospheric aerosol samples during southern-eastern wind directions (from the sea). NaNO_3 is a successor when NaCl is altered, i.e. after long range transport.

By means of the molar mass, the mass of the salts and the density of the chemical compounds the volume of predominating compounds on each impactor stage was calculated. As the analysis of the material on each sample was done in the laboratory under 52% RH it was assumed that a certain amount of water was attracted to each sample. Based on the theoretical hygroscopic growth of the model salts at 52% RH (Tang and Munkelwitz, 1994), the amount of water during weighing was calculated. To

Hygroscopic growth of urban aerosol particles in Beijing

J. Meier et al.

Title Page

Abstract

Introduction

Conclusions

References

Tables

Figures

◀

▶

◀

▶

Back

Close

Full Screen / Esc

Printer-friendly Version

Interactive Discussion



obtain the dry weight of a sample, the water mass attracted to the particle at RH=52% was subtracted from the total particle mass. In addition, the average particle density of 1.7 g cm^{-3} was used to calculate the total dry particle volume for each impactor sample. Based on the total dry volume, the volume of soluble (composed salts) and insoluble material (EC+OM) was calculated. Here, the part of soluble and insoluble volume from total volume was used as volume fraction $e_{\text{stage}}^{\text{salt}}$ or $e_{\text{stage}}^{\text{insoluble}}$. Then, the hygroscopic growth of an atmospheric particle with a mixed chemical composition based on the Zdanovskii-Stokes-Robinson-Relation (ZSR) (Zdanovskii, 1948; Stokes and Robinson, 1966) was determined. A growth factor of GF=1 was used for the non-soluble volume fraction at every relative humidity. As the characteristic growth of the observed soluble chemical compounds is known, the average growth factor (CHGF) for each impactor stage sample was calculated. The order of chemical compounds formed by the model was changed in six different runs and is listed below. The first composition is assumed to be most available, followed by the second one and so on (Table 1).

4 Results

4.1 Meteorological overview

During the measurement campaign between 17 and 25 January 2005, the meteorological situation in northern China underwent several changes, which led to changes in the observed particle mass concentration and chemical composition. Figure 1 presents the particle mass size distribution and the total particle mass (PM_{10} : $D_{\text{aero}} \leq 1 \mu\text{m}$) calculated by means of the particle number size distribution of dry particles (measured with TDMPs) and assuming of mean particle density of 1.7 g cm^{-3} based on chemical data. In addition, the measured temperature and relative humidity as well as wind speed and wind direction are shown in Fig. 1. Based on meteorological conditions the whole measurement period was classified into three time periods indicating the observation of different air masses. In the course of this study three time periods are named as A1,

Hygroscopic growth of urban aerosol particles in Beijing

J. Meier et al.

Title Page

Abstract

Introduction

Conclusions

References

Tables

Figures

◀

▶

◀

▶

Back

Close

Full Screen / Esc

Printer-friendly Version

Interactive Discussion



A2 and A3.

4.1.1 Air mass A1 (relatively clean)

Between 17 January, 12:00 and 20 January, 19:00, relatively clean air masses were transported from north-western regions, the less populated and industrialised part of China, to Beijing (Fig. 2, red). The transport of cleaner air masses from the northern regions was also described by Wehner et al. (2008) during a 2-year-study in Beijing. The aerosol was either of continental clean or urban polluted character. Since Beijing is a constant emitter of particles and precursor gases during day and nighttime, the accumulation of primary and secondary particle number and mass depends on the transport time of the air mass over the city area. During daytime, the wind speed was much higher than during nighttime (maximum day: 7.7 m s^{-1} ; maximum night: 0.12 m s^{-1}). Due to calm winds, the accumulation of urban aerosol was thus greatest during nighttime. The particle mass concentration was highest for the last two nights. Mainly clean continental aerosol was observed during daytime and at the beginning of the period. The maximum particle mass concentration was determined to $176 \mu\text{g m}^{-3}$ (Fig. 1). Air mass A1 was characterized as dry, with an average relative humidity of 28%.

4.1.2 Air mass A2 (polluted)

The second time period (20 January, 19:00–24 January, 01:00) shows transport of air masses mainly from southern directions to Beijing (Fig. 2, green), where the population is very dense and the industrialisation very distinct. The accumulation of aerosol number and mass was enhanced during transport due to the low wind speed (average: 1 m s^{-1}) as it was also described as cluster 5 and 6, respectively, by Wehner et al. (2008). The aerosol measured in Beijing is thus a mixture of accumulated regional and urban pollution. During the entire time period, the particle mass concentrations increased from day to day with maxima during nighttime in the beginning of the period

Hygroscopic growth of urban aerosol particles in Beijing

J. Meier et al.

Title Page

Abstract

Introduction

Conclusions

References

Tables

Figures

◀

▶

◀

▶

Back

Close

Full Screen / Esc

Printer-friendly Version

Interactive Discussion



(Fig. 1). At the end of this period, the particle mass concentration reached a maximum value of $520 \mu\text{g m}^{-3}$. The relative humidity increased during the whole time period with a maximum of 62% shortly before the air mass change.

4.1.3 Air mass A3 (relatively clean)

5 A sudden change of the meteorological conditions initiated an abrupt decrease of particle mass concentration, which indicated the beginning of the third air mass period from 24 January, 01:00 to 25 January, 10:00 (Fig. 1). The relatively clean air mass (Fig. 2, blue) reached Beijing from northerly directions passing the mountains. Due to a foehn effect, the relative humidity decreased rapidly from 62% to 24%. In the beginning of
10 the period, the wind speed increased from 1 m s^{-1} to nearly 6 m s^{-1} leading to lower particle mass concentrations (maximum: $229 \mu\text{g m}^{-3}$) of a clean continental air mass. Later, the wind calmed down to around 2 m s^{-1} causing accumulation of the particle mass concentration of mainly urban origin.

4.2 Impactor sampling events

15 Three MOUDI samples of atmospheric particles for chemical analysis were taken during the entire field study one each during air mass period 1 and 2, and one in the overlap period between air mass 2 and air mass 3. The samples were taken from mid-day of 17 January to midday of 18 January (I1), from 22 January, 14:00, to 23 January, 14:00 (I2) and from 23 January, 16:00 to midday of 24 January (I3). The first two im-
20 pactor sampling periods (I1 and I2) are representative for the conditions found during air mass A1 and A2, respectively. Impactor sampling period I3, however, represents a mixture of the conditions during A2 and A3.

In Fig. 3 the mass fractions of the different chemical species for all time periods within ten aerodynamic diameters ranges are shown. Generally, coarse particles
25 ($D_{\text{aero}}=1.8 \mu\text{m}$ and larger) contained mostly unspecified material. This is associated mainly with insoluble minerals, such as silicates and iron oxides. Water is included in

Hygroscopic growth of urban aerosol particles in Beijing

J. Meier et al.

Title Page

Abstract

Introduction

Conclusions

References

Tables

Figures

◀

▶

◀

▶

Back

Close

Full Screen / Esc

Printer-friendly Version

Interactive Discussion



Hygroscopic growth of urban aerosol particles in Beijing

J. Meier et al.

Title Page

Abstract

Introduction

Conclusions

References

Tables

Figures

◀

▶

◀

▶

Back

Close

Full Screen / Esc

Printer-friendly Version

Interactive Discussion



the category “unspecified material”. Fine particles ($D_{\text{aero}} \leq 1 \mu\text{m}$) contained an increasing fraction of inorganic ions as well as OM and EC with decreasing particle size. The main difference between impactor sampling periods I1, I2 and I3 in chemical particle composition is caused by their different air mass origin. Figure 4 shows back trajectories for the three measurement periods. In Table A1, a short overview of the total mass, the mass of inorganic ions, OM, EC and unspecified material is given. In addition the ratio between OM and EC and soluble and insoluble material, respectively, for three diameter ranges is listed.

4.2.1 Impactor sampling period I1 (relatively clean)

The first sampling period (17 January, 12:00–18 January, 12:00) is characterized by the cleanest air mass of all three impactor sampling periods. During I1, the air mass was transported from western and north-western regions to Beijing (Fig. 4, red) (total particle mass: $31 \mu\text{g m}^{-3}$ for $0.1\text{--}10 \mu\text{m}$ particles). The ratio of OM to EC is for all three size ranges larger than 2 (Table A1). The higher the OM/EC ratio the more aged the aerosol is due to accumulation of OM from the gas phase (Cao et al., 2003). The influence of freshly emitted aerosol was relatively small for this impactor sampling period. The aerosol was characterized as clean continental as shown in Fig. 1.

4.2.2 Impactor sampling period I2 (polluted)

The second sampling period (22 January, 14:00–23 January, 14:00) can be characterized as very polluted. The total mass of this particle sample was $275 \mu\text{g m}^{-3}$ ($D_{\text{aero}} = 0.1\text{--}10 \mu\text{m}$). As described above and shown in Fig. 4, the air mass arrived slowly from the south transporting probably a significant amount of aerosol mass from regional sources. Additionally, the aerosol accumulation was enhanced in the Beijing area resulting in a mixture of regional and local urban aerosol. The OM/EC ratio of approximately one for $D_{\text{aero}} \geq 0.18 \mu\text{m}$ supports this interpretation. Low OM/EC ratios are generally connected to direct vehicular emissions (Viidanoja et al., 2002).

4.2.3 Impactor sampling period I3 (mixed)

The last period (23 January, 16:00–24 January, 12:00) unfortunately overlapped air mass A2 and A3. As shown in Fig. 1, air mass A2 dominated the total aerosol mass concentration compared to A3. This fact underlines that the particle mass was mainly collected during the last hours of A2 (total particle mass: $222 \mu\text{g m}^{-3}$ for 0.1–10 μm particles). The calculated mass fraction (from TDMPs measurements) of air mass A2 was approximately 90% of the total mass measured during impactor sampling period I3. The OM/EC ratios differ only slightly from I2 indicating a mixture of regional and urban influence.

4.3 Hygroscopic particle growth factors

4.3.1 Descriptive hygroscopic growth factors

The calculated descriptive hygroscopic growth factors (DHGFs) based on the measurements of TDMPs and H-DMPS are illustrated in Fig. 5 and listed in Table A2. The DHGFs were time-averaged for each air mass and relative humidity (RH=55%, 77% and 90%). The error bars indicate the variation of the growth factors dependent on fluctuations of RH during measurement. In general, the calculated descriptive hygroscopic growth factors are relatively low. Noticeable is the range of DHGFs at the smallest particle diameters. They are similar and do not show significant differences in dependence on investigated air mass.

Air Mass A1 reached Beijing from northwesterly directions with relatively high wind speeds during daytime and low wind speeds during nighttime. Here, unfortunately, only H-DMPS measurements during nighttime with an increased accumulation of the urban aerosol were available. The lowest growth factors were determined compared to the other two time periods (Fig. 5). At relative humidities 55% and 77%, the shapes of the curves are similar showing two maxima at $D_p=110$ and 250 nm. The DHGF at RH=90% has got however only one maximum at $D_p=118$ nm (DHGF=1.33 (0.03)).

Title Page

Abstract

Introduction

Conclusions

References

Tables

Figures

◀

▶

◀

▶

Back

Close

Full Screen / Esc

Printer-friendly Version

Interactive Discussion



Hygroscopic growth of urban aerosol particles in Beijing

J. Meier et al.

Title Page

Abstract

Introduction

Conclusions

References

Tables

Figures

◀

▶

◀

▶

Back

Close

Full Screen / Esc

Printer-friendly Version

Interactive Discussion



For air mass A2, the descriptive hygroscopic growth factors were higher compared to A1. The hygroscopic growth factors were similar for particle sizes greater than 80 nm at RH=55% and 77%. The maximum growth factor of 1.40 (0.03) was observed for the size range 200–300 nm at RH=90%, which can be related to an increased accumulation of secondary soluble aerosol compounds during transport. Air mass A2 was influenced strongly by the regional aerosol and accumulated urban aerosol due to the very low wind speeds.

During air mass A3, the shape of the DHGF curves changed in comparison to A2. For all three relative humidities, the growth factors of particles larger than 200 nm are lower, which is probably due to because of a lower fraction of soluble material in this size range. The maximum of the growth factors of 1.40 (0.03) occurred at 150 nm. The reason for this change is the less polluted air, i.e. less aged aerosol compared to air mass A2.

4.3.2 Comparison with H-TDMA data

The hygroscopic growth of selected particle diameters of 30, 50, 80, 150, 250 and 350 nm was determined at RH=90% by means of the H-TDMA. Figure 5 includes these results for the discussed time periods of A1, A2 and A3. Growth factors from the H-TDMA measurements are in good agreement with those measured with the H-DMPS/TDMPS technique. In general, H-TDMA growth factors are somewhat higher than the DHGF but the shape of the growth curves at RH=90% is well represented. For A1, we have a clear shift, the mean difference between the DHGF of H-DMPS/TDMPS and the \overline{GF} of the H-TDMA is 0.07, but with better agreement (0.05) for larger particles ($D_p \geq 150$ nm). During the high polluted period A2, the mean discrepancy between these two methods is, like during A1, 0.07 but remarkably better (0.03) for $D_p \geq 150$ nm. The smallest differences between measured (H-TDMA) \overline{GF} and calculated (H-DMPS/TDMPS) DHGF was determined for air mass A3. The mean difference of DHGF is 0.05 and 0.01 for particles with $D_p \geq 150$ nm. The increasing correlation

Hygroscopic growth of urban aerosol particles in Beijing

J. Meier et al.

between the calculated and the measured growth factors with increasing particle diameter is illustrated in Fig. 6. Here, growth factors were compared when data from the H-TDMA, the H-DMPS and the TDMPs were available within the same hour. The correlation coefficient between DHGF and \overline{GF} is plotted showing that with increasing particle diameter the agreement between the compared methods increases too (Table 2). Overall, hygroscopic growth factors of less and more hygroscopic particles observed within this study were slightly smaller in comparison to those found at several other urban sites (Swietlicki et al., 2008). This finding indicates that insoluble carbonaceous matter was a significant component of all particle groups of the sub-micrometer Beijing aerosol during wintertime. This behavior was eminently observed for particles with $D_p=150$ nm.

4.4 CHGFs from chemical composition

Based on the chemical analysis of the MOUDI samples, hygroscopic growth factors were calculated by a solubility model. Several model runs were carried out to calculate hygroscopic growth factors; as described in 3.3. Based on the sampling periods I1 to I3, the mean descriptive hygroscopic growth factors at RH=90% (based on TDMPs and H-DMPS measurements) were calculated for the same time. It has to be noticed that for the first period I1 only one reliable DHGF from the H-DMPS/TDMPs measurement was available to compare with the model results. For I2 and I3 an average of 13 and 9 DHGF results, respectively, were taken into account. In Fig. 7 these mean DHGFs are shown in comparison with the model results (see also Tables A2 and A4). For a better overview, only the runs (as described above) 1, 3 and 6 are presented. The results of the runs 2, 4 and 5 were found between those presented here. Generally, the DHGFs and the CHGFs show a partly agreement only. Certainly, there are cases of over- and underestimation in the overlap region ($D_p=44$ –800 nm), but the difference between DHGF and CHGF is within the uncertainty range of the solubility model based on the uncertainty of chemical analysis. Obviously, no run representing a defined composition of inorganic chemical compounds fits with all measured DHGFs for all three periods.

Title Page

Abstract

Introduction

Conclusions

References

Tables

Figures

◀

▶

◀

▶

Back

Close

Full Screen / Esc

Printer-friendly Version

Interactive Discussion



But, in principle the shape of the curves is well represented by the model results, especially during the third period. Furthermore, the error for the CHGFs for lower ion concentrations (as in the case of I1) is assumed to be higher in comparison to the error for the highly polluted events (I2 and I3).

5 In case of impactor sampling period I1 (Fig. 7, I1), the results of the model correspond with the DHGF although there is just one measurement to compare with, which might however not be representative. Nevertheless, there is a wide range between the model results, especially for the larger particle sizes. The discrepancies between the DHGFs and the CHGFs for the entire diameter range are 0.06 (Run 1), 0.08 (Run 2),
10 0.03 (Run 3, Run 4), 0.10 (Run 5) and 0.13 (Run 6) and therefore strongly dependent on the chosen chemical composition. For particles larger than 100 nm the discrepancies vary between 0.04 and 0.15. During the first sampling period, the concentrations of NO_3^- and NH_4^- for smaller particle diameters were low compared to the other two periods leading in principle to larger uncertainties.

15 The model runs for impactor sampling period I2 (Fig. 7, I2) do show differences between the different model runs and the measurements. The maximum of the DHGF distribution is not well represented by the model. For particles larger than 100 nm, the runs underestimate the DHGF. However, the general tendency of increasing growth for smaller and decreasing growth for larger particles is reflected by all model calculations.
20 The particle mass concentration was largest during this period (Table A1), but the fraction of the unknown material was also very large, which increased the uncertainty in this case. For the unknown particle fraction, we used a growth factor of one leading to a decreased mean CHGF, which could be a reason for the underestimation. The discrepancies between the DHGF and the CHGF are 0.05–0.06 (60–800 nm particles) and 0.04–0.07 ($D_p \geq 100$ nm), respectively, less than during I1.
25

The comparison between the model runs (Fig. 7, I3) and the measurements is best for the last impactor sampling period I3. There are no significant differences between the model results (CHGFs) and the measured DHGFs for particles with diameters larger than 100 nm. The mean discrepancies vary between 0.05 and 0.06 (70–400 nm

Hygroscopic growth of urban aerosol particles in Beijing

J. Meier et al.

Title Page

Abstract

Introduction

Conclusions

References

Tables

Figures

◀

▶

◀

▶

Back

Close

Full Screen / Esc

Printer-friendly Version

Interactive Discussion



particles). The agreement for particles larger than 100 nm is still better with 0.02–0.03. The chemical composition of the third impactor sampling period was mainly determined by the strong pollution during observation of air mass A2 indicating that the chemical composition was more homogeneous and the model results were probably better comparable with the measured hygroscopic growth factors.

5 Conclusions

Humidified particle number size distributions (D_p range 22–900 nm; RH up to 90%), dry number size distributions (D_p range 3–900 nm), hygroscopic growth factors (RH 90%), and the chemical composition of aerosol particles were determined simultaneously in the urban atmosphere of Beijing, China, in January 2005. The data set is complementary in the sense that for the same parameter, the hygroscopic growth factor of ambient aerosol particles, three alternative methods could be compared quantitatively.

The measurement period was divided into three sub-periods (termed “air masses” hereafter) on the basis of a meteorological evaluation and the calculated particle mass concentrations ($D_p < 1 \mu\text{m}$). The air mass A1 with an average mass concentration of $44 \mu\text{g m}^{-3}$ represented the relatively “clean” continental background air that is typically encountered in Beijing under northeasterly winds (Wehner et al., 2008). Here, the chemical particle analysis indicated low fractions of soluble inorganic components and elemental carbon compared to organic matter, indicating the presence of secondary organic aerosol. Air mass A2, in contrast, captured the massive influence of the anthropogenic sources within the North China Plain occurring under slow southerly winds, and was characterised by a total mass concentration of $207 \mu\text{g m}^{-3}$. The chemical composition indicated a stronger contribution of soluble inorganic components, elemental carbon and organic matter concentrations. During a third air mass A3, conditions similar to air mass A1 were repeated.

H-DMPS and TDMPS particle number size distributions were evaluated using the summation method (Birmili et al., 2009) from which descriptive hygroscopic growth

Hygroscopic growth of urban aerosol particles in Beijing

J. Meier et al.

Title Page

Abstract

Introduction

Conclusions

References

Tables

Figures

◀

▶

◀

▶

Back

Close

Full Screen / Esc

Printer-friendly Version

Interactive Discussion



Hygroscopic growth of urban aerosol particles in Beijing

J. Meier et al.

Title Page

Abstract

Introduction

Conclusions

References

Tables

Figures

◀

▶

◀

▶

Back

Close

Full Screen / Esc

Printer-friendly Version

Interactive Discussion



factors (DHGFs) were derived as a function of particle size. The DHGFs determined for the three air masses were found to be relatively low compared to observations of the regional aerosol near Beijing in summer (Achtert et al., 2009) or in atmospheres elsewhere (Swietlicki et al., 2008). The lowest DHGFs (at 90% RH) were observed during air mass A1 with a maximum of 1.33 (uncertainty: 0.03) at $D_p=118$ nm. In air mass A2, the maximum DHGF increased to 1.40 (0.03) for 200–300 nm particles. Very similar values prevailed during the observation of air mass A3.

The descriptive hygroscopic growth factors derived from the H-DMPS/TDMPS and the hygroscopic growth factors from the H-TDMA for concurrent measurements agreed within 0.07 (during air mass A1), 0.06 (during air mass A2) and 0.05 (during air mass A3). The deviation between the two methods in terms of DHGF became smaller with increasing particle diameter, manifested by increasing correlation coefficients of 0.28, 0.64, 0.86 and 0.89 for the dry diameters 50, 150, 250 and 350 nm. We interpret the reduced correlation coefficients at lower particle sizes as a limitation of the summation method, where size distributions involving large particle numbers are subtracted from each other. Since the association of dry and humidified particle number segments starts at the upper end of the size distributions, accidental measurement errors can propagate more easily into DHGF at the lower distribution end (Birmili et al., 2009) while the values above 70 nm remain almost unaffected.

As a third method, hygroscopic growth factors (CHGFs) were calculated for 90% RH on the basis of chemical particle composition gathered from three MOUDI impactor samples (I1, I2, I3). Each impactor sample encompassed between five and six size fractions in the sub-micrometer range. Different growth model versions were initialised with these data, varying with the particular selection of soluble species that were included in the model calculations. During impactor period I1 (clean continental air; relatively low DHGFs), modelled CHGFs exceeded the experimental values but stayed within a mean discrepancy of 0.03–0.13 (depending on the chosen chemical composition) of the DHGF data. During impactor period I2, marked by higher DHGFs, a better agreement was found, with a mean discrepancy of 0.05–0.06. The best agreement

was found for the period I3, with a mean deviation of 0.02–0.03 for 100–400 nm particles. That the methods agree with respect to their trend in CHGF as a function of particle size, manifesting a maximum CHGF in the lower accumulation mode (100–300 nm), even if the absolute values are not matched. The observed divergences in their absolute values seem to be plausible in view of the uncertainties involved in the measurements and evaluation techniques as well as the restriction of initializing a detailed growth model with chemical particle data that is limited to several soluble ions and a few bulk classes of compounds.

Our work demonstrates the capability as well as the limitations of different methods using physical instruments (H-DMPS/TDMPS, H-TDMA), or chemical analysis of impactor samples combined with a solubility model to qualitatively determine the hygroscopic growth of environmental particles as a function of particle size. The data collected in the city of Beijing in wintertime showed lower growth factors than expected, which is likely a result of the relatively high carbonaceous aerosol fraction during our observation periods. Our results are therefore relevant for an accurate prediction of aerosol radiative effects as well as visibility impacts in this socio-economically rapidly changing region.

Acknowledgements. This work was supported by DFG (Deutsche Forschungsgemeinschaft) grants WI 1449/9-1 and WI 1449/9-2. The data evaluation was supported by the European Integrated project on Aerosol Cloud Climate and Air Quality Interactions (EUCAARI), coordinated by the University of Helsinki, Finland.

Hygroscopic growth of urban aerosol particles in Beijing

J. Meier et al.

Title Page

Abstract

Introduction

Conclusions

References

Tables

Figures

◀

▶

◀

▶

Back

Close

Full Screen / Esc

Printer-friendly Version

Interactive Discussion



References

- Achtert, P., Birmili, W., Nowak, A., Wehner, B., Wiedensohler, A., Takegawa, N., Kondo, Y., Miyazaki, Y., Hu, M., and Zhu, T.: Hygroscopic growth of tropospheric particle number size distributions over the North China Plain, *J. Geophys. Res.*, in press, 2009. 6893, 6909
- 5 Bergin, M. H., Cass, G. R., Xu, J., Fang, C., Zeng, L. M., Yu, T., Salmon, L. G., Kiang, C. S., Zhang, Y. H., and Chameides, W. L.: Aerosol radiative, physical, and chemical properties in Beijing during June 1999, *J. Geophys. Res.*, 106(D16), 17969–17980, 2001. 6891
- Birmili, W., Stratmann, F., and Wiedensohler, A.: Design of a DMA-based size Spectrometer for a large Particle Size Range and Stable Operation, *J. Aerosol Sci.*, 30(4), 549–553, 1999.
- 10 6895
- Birmili, W., Schwirn, K., Nowak, A., Petäjä, T., Joutsensaari, J., Rose, D., Wiedensohler, A., Hämeri, K., Aalto, P., Kulmala, M., and Boy, M.: Hygroscopic growth of atmospheric particle number size distributions in the Finnish boreal forest region, *Boreal Environ. Res.*, in press, 2009. 6895, 6898, 6908, 6909
- 15 Brüggemann, E. and Rolle, W.: Changes of some components of precipitation in East Germany after the unification, *Water Air Soil Poll.*, 107, 1–23, 1998.
- Cao, J. J., Lee, S. C., Ho, K. F., Zhang, X. Y., Zou, S. C., Fung, K., Chow, J. C., and Watson, J. G.: Characteristics of carbonaceous aerosol in Pearl River Delta Region, China during 2001 winter period, *Atmos. Environ.*, 37(11), 1451–1460, 2003. 6903
- 20 Charlson, R. J. and Heintzenberg, J.: *Aerosol forcing of climate*, John Wiley and Sons Ltd., New York, 416 pp., 1995. 6892
- Cheng, Y. F., Wiedensohler, A., Eichler, H., Heintzenberg, J., Tesche, M., Ansmann, A., Wendisch, M., Su, H., Althausen, D., Herrmann, H., Gnauk, T., Brüggemann, E., Hu, M., and Zhang, Y. H.: Relative humidity dependence of aerosol optical properties and direct radiative forcing in the surface boundary layer at Xinken in Pearl River Delta of China: An observation based numerical study *Atmos. Environ.*, 42, 6373–6397, 2009. 6893
- 25 Cocker, D., Whitlock, N., Flagan, R., and Seinfeld, J. H.: Hygroscopic properties of Pasadena, California aerosol, *Aerosol Sci. Tech.*, 35(2), 637–647, 2001. 6892
- Draxler, R. R. and Hess, G. D.: Description of the HYSPLIT-4 modeling system, NOAA Technical Memorandum ERL ARL-224, 25 pp., 2004. 6922, 6924
- 30 Eichler, H., Cheng, Y. F., Birmili, W., Nowak, A., Wiedensohler, A., Brüggemann, E., Gnauk, T., Herrmann, H., Althausen, D., Ansmann, A., Engelmann, R., Tesche, M., Wendisch, M.,

ACPD

9, 6889–6927, 2009

Hygroscopic growth of urban aerosol particles in Beijing

J. Meier et al.

Title Page

Abstract

Introduction

Conclusions

References

Tables

Figures

◀

▶

◀

▶

Back

Close

Full Screen / Esc

Printer-friendly Version

Interactive Discussion



**Hygroscopic growth
of urban aerosol
particles in Beijing**

J. Meier et al.

Title Page

Abstract

Introduction

Conclusions

References

Tables

Figures

◀

▶

◀

▶

Back

Close

Full Screen / Esc

Printer-friendly Version

Interactive Discussion

Zhang, Y. H., Hu, M., Liu, S., and Zeng, L. M.: Hygroscopic properties and extinction of aerosol particles at ambient relative humidity in South-Eastern China, *Atmos. Environ.*, 42, 6321–6334, 2008. 6893, 6895

Fenger, J.: Urban air quality, *Atmos. Environ.*, 33(29), 4877–4900, 1999. 6891

5 Ferron, G., Karg, E., Busch, B., and Heyder, J.: Ambient particles at an urban, semi-urban and rural site in Central Europe: Hygroscopic properties, *Atmos. Environ.*, 39(2), 343–352, 2005. 6892

Florig, H. K.: China's air pollution risks, *Environ. Sci. Technol.*, 31(6), 274A–279A, 1997. 6891
Jinhuan, Q. and Liquan, Y.: Variation characteristics of atmospheric aerosol optical depths and
10 visibility in North China during 1980–1994, *Atmos. Environ.*, 34(4), 603–609, 2000. 6892

Mage, D., Ozolins, G., Peterson, P., Webster, A., Orthofer, R., Vandeweerd, V., and Gwynne, M.: Urban air pollution in megacities of the world, *Atmos. Environ.*, 30(5), 681–686, 1996. 6891

Marple, V. A., Rubow, K. L., and Behm, S. M.: A Microorifice Uniform Deposit Impactor (MOUDI): Description, calibration, and use, *Aerosol Sci. Tech.*, 14, 434–446, 1991. 6896

15 Massling, A., Stock, M., Wehner, B., Wu, Z. J., Hu, M., Brüggemann, E., Gnauk, T., Herrmann, H., and Wiedensohler, A.: Size segregated water uptake of the urban submicrometer aerosol in Beijing, *Atmos. Environ.*, 43(8), 1578–1589, 2009. 6893

Massling, A., Stock, M. and Wiedensohler, A.: Diurnal, weekly, and seasonal variation of hygroscopic properties of submicrometer urban aerosol particles, *Atmospheric Environment*, 39, 3911–3922, 2005. 6892, 6896

20 Maßling, A., Wiedensohler, A., Busch, B., Neusüß, C., Quinn, P., Bates, T., and Covert, D.: Hygroscopic properties of different aerosol types over the Atlantic and Indian Oceans, *Atmos. Chem. Phys.*, 3, 1377–1397, 2003, <http://www.atmos-chem-phys.net/3/1377/2003/>. 6898

25 McMurry, P. and Stolzenburg, M.: On the sensitivity of particle size to relative humidity for Los Angeles aerosols, *Atmos. Environ.*, 23(2), 497–507, 1989. 6892

Neusüss, C., Pelzing, M., Plewka, A., and Herrmann, H.: A new analytical approach for size-resolved speciation of organic compounds in atmospheric aerosol particles: Methods and first results, *J. Geophys. Res.*, 105(D4), 4513–4527, 2000.

30 Rader, D. J. and McMurry, P. H.: Application of the Tandem Differential Mobility Analyzer to studies of droplet growth or evaporation, *J. Aerosol Sci.*, 17(5), 771–787, 1986. 6896

Stokes, R. H. and Robinson, R. A.: Interactions in Aqueous Nonelectrolyte Solutions, I. Solute-Solvent Equilibria, *J. Phys. Chem.-US*, 70, 2126–2130, 1966. 6900

- Stratmann, F. and Wiedensohler, A.: A new data inversion algorithm for DMPS-measurements, *J. Aerosol Sci.*, 27(S1), S339–S340, 1996. 6895
- Sugimoto, N., Uno, I., Nishikawa, M., Shimizu, A., Matsui, I., Dong, X., Chen, Y., and Quan, H.: Record heavy Asian dust in Beijing in 2002: Observations and model analysis of recent events, *Geophys. Res. Lett.*, 30(12), 1640, doi:10.1029/2002GL016349, 2003. 6892
- Swietlicki, E., Hansson, H.-C., Hämeri, K., Svenningsson, B., Massling, A., McFiggans, G., McMurry, P. H., Petäjä, T., Tunved, P., Gysel, M., Topping, D., Weingartner, E., Baltensperger, U., Rissler, J., Wiedensohler, A., and Kulmala, M.: Hygroscopic properties of submicrometer atmospheric aerosol particles measured with H-TDMA instruments in various environments – a review, *Tellus B*, 60(3), 432–469, 2008. 6892, 6898, 6906, 6909
- Tang, A., Zhuang, G., Wang, Y., Yuan, H., and Sun, Y.: The chemistry of precipitation and its relation to aerosol in Beijing, *Atmos. Environ.*, 39, 3397–3406, 2005. 6891
- Tang, I. N. and Munkelwitz, H. R.: Water activities, densities, and refractive indices of aqueous sulfates and sodium nitrate droplets of atmospheric importance, *J. Geophys. Res.*, 99(D9), 18801–818808, 1994. 6899
- Tang, I., Wong, W., and Munkelwitz, H. R.: The relative importance of atmospheric sulfates and nitrates in visibility reduction, *Atmos. Environ.*, 15(12), 2463–2471, 1981. 6892
- Turpin, B. J. and Lim, H.-J.: Species contributions to $PM_{2.5}$ mass concentrations: Revisiting common assumptions for estimating organic mass, *Aerosol Sci. Tech.*, 35, 602–610, 2001. 6899
- VDI 2465 Part 2: Measurement of soot (ambient air), thermographic determination of elemental carbon after thermal desorption of organic carbon, *VDI/DIN-Handbuch Reinhaltung der Luft, Band 4*, 18 pp., 1999. 6897
- Viidanoja, J., Sillanpää, M., Laakia, J., Kerminen, V.-M., Hillamo, R., Aarnio, P., and Koskentalo, T.: Organic and black carbon in $PM_{2.5}$ and PM_{10} : 1 year of data from an urban site in Helsinki, Finland, *Atmos. Environ.*, 36, 3183–3193, 2002. 6903
- Wehner, B., Birmili, W., Ditas, F., Wu, Z., Hu, M., Liu, X., Mao, J., Sugimoto, N., and Wiedensohler, A.: Relationships between submicrometer particulate air pollution and air mass history in Beijing, China, 2004–2006, *Atmos. Chem. Phys.*, 8, 6155–6168, 2008, <http://www.atmos-chem-phys.net/8/6155/2008/>. 6892, 6908
- Wehner, B., Wiedensohler, A., Tuch, T., Wu, Z. J., Hu, M., Slanina, J., and Kiang, C. S.: Variability of the aerosol number size distribution in Beijing, China: New particle formation, dust storms, and high continental background, *Geophys. Res. Lett.*, 31, L22108,

Hygroscopic growth of urban aerosol particles in Beijing

J. Meier et al.

Title Page

Abstract

Introduction

Conclusions

References

Tables

Figures

◀

▶

◀

▶

Back

Close

Full Screen / Esc

Printer-friendly Version

Interactive Discussion



doi:10.1029/2004GL021596, 2004. 6892

Wu, Z., Hu, M., Liu, S., Wehner, B., Bauer, S., Massling, A., Wiedensohler, A., Petäjä, T., Dal Maso, M., and Kulmala, M.: New particle formation in Beijing, China: Statistical analysis of a one-year-dataset, *J. Geophys. Res.*, 112, D09209, doi:10.1029/2006JD007406, 2007. 6892

5 Xu, X., Gao, J., Dockery, D. W., and Chen, Y.: Air pollution and daily mortality in residential areas of Beijing, China, *Arch. Environ. Health*, 49(4), 216–222, 1994. 6891

Zdanovskii, A. B.: New methods of calculating solubilities of electrolytes in multicomponent systems, *Zh. Fiz. Khim.*, 22, 1475–1485, 1948. 6900

10 Zhang, R., Wang, M., Zhang, X., and Zhu, G.: Analysis on the chemical and physical properties of particles in a dust storm in spring in Beijing, *Powder Technol.*, 137(1–2), 77–82, 2003. 6892

ACPD

9, 6889–6927, 2009

Hygroscopic growth of urban aerosol particles in Beijing

J. Meier et al.

Title Page

Abstract

Introduction

Conclusions

References

Tables

Figures

◀

▶

◀

▶

Back

Close

Full Screen / Esc

Printer-friendly Version

Interactive Discussion



Hygroscopic growth of urban aerosol particles in Beijing

J. Meier et al.

Table 1. Order of different chemical compounds at six runs for the calculation of the hygroscopic growth factor.

	1. Composition	2. Composition	3. Composition	4. Composition
Run 1	NH_4NO_3	$(\text{NH}_4)_2\text{SO}_4$	H_2SO_4	
Run 2	$(\text{NH}_4)_2\text{SO}_4$	NH_4NO_3	NaCl	
Run 3	$(\text{NH}_4)_2\text{SO}_4$	NH_4NO_3	NaNO_3	
Run 4	NH_4NO_3	$(\text{NH}_4)_2\text{SO}_4$	NaNO_3	
Run 5	$(\text{NH}_4)_2\text{SO}_4$	NH_4NO_3	H_2SO_4	NaCl
Run 6	NH_4NO_3	$(\text{NH}_4)_2\text{SO}_4$	H_2SO_4	NaCl

Title Page

Abstract

Introduction

Conclusions

References

Tables

Figures

◀

▶

◀

▶

Back

Close

Full Screen / Esc

Printer-friendly Version

Interactive Discussion



**Hygroscopic growth
of urban aerosol
particles in Beijing**

J. Meier et al.

Table 2. Correlation coefficients of hygroscopic growth factors between H-TDMA and H-DMPS/TDMPS results for four different particle diameters.

Particle Diameter [nm]	50	150	250	350
Correlation Coefficient R	0.278	0.642	0.859	0.889

[Title Page](#)[Abstract](#)[Introduction](#)[Conclusions](#)[References](#)[Tables](#)[Figures](#)[I◀](#)[▶I](#)[◀](#)[▶](#)[Back](#)[Close](#)[Full Screen / Esc](#)[Printer-friendly Version](#)[Interactive Discussion](#)

Hygroscopic growth of urban aerosol particles in Beijing

J. Meier et al.

Table A1. Total mass and analysed mass of inorganic ions, EC, OM and the unspecified material. Additionally the ratio of OM/EC and soluble/insoluble material for the three impactor sampling periods (I1, I2, I3) with the MOUDI.

Time Period	Aerodynamic							
	Diameter [μm]	Total Mass [$\mu\text{g m}^{-3}$]	Inorganic Ions [$\mu\text{g m}^{-3}$]	OM [$\mu\text{g m}^{-3}$]	EC [$\mu\text{g m}^{-3}$]	Unspecified [$\mu\text{g m}^{-3}$]	OM/EC	Soluble/Insoluble
I1	0.1	0.828	0.278	0.331	0.086	0.132	3.834	0.506
(17-01-2005 12:00	0.18–0.32	8.473	2.541	2.782	0.566	1.537	4.911	0.520
–18-01-2005 12:00)	0.56–10	17.934	17.934	1.958	0.800	11.842	2.448	1.228
I2	0.1	7.711	2.457	2.011	0.514	2.729	3.915	0.468
(22-01-2005 14:00	0.18–0.32	116.681	41.039	19.001	18.434	38.207	1.031	0.543
–23-01-2005 14:00)	0.56–10	150.280	24.467	13.631	12.164	100.018	1.121	0.194
I3	0.1	3.583	1.436	0.860	0.418	0.870	2.058	0.669
(23-01-2005 16:00	0.18–0.32	56.824	22.497	11.435	7.343	15.549	1.557	0.655
–24-01-2005 12:00)	0.56–10	161.391	31.426	15.537	12.846	101.583	1.210	0.242

Title Page

Abstract

Introduction

Conclusions

References

Tables

Figures

◀

▶

◀

▶

Back

Close

Full Screen / Esc

Printer-friendly Version

Interactive Discussion



Hygroscopic growth of urban aerosol particles in Beijing

J. Meier et al.

Table A2. Hygroscopic descriptive growth factors, calculated based on the number size distributions of TDMPs and H-DMPS measurements for three different time periods (A1, A2, A3) at a relative humidity of RH=55%, 77% and 90% and for the impactor sampling periods (I1, I2, I3) at RH=90%.

D_p [nm]	A1 (17-01-2005 12:00 –20-01-2005 19:00)			A2 (20-01-2005 19:00 –24-01-2005 01:00)			A3 (24-01-2005 01:00 –25-01-2005 10:00)			I1 (17-01-2005 12:00 –18-01-2005 12:00)	I2 (22-01-2005 14:00 –23-01-2005 14:00)	I3 (23-01-2005 16:00 –24-01-2005 12:00)
	RH=55%	RH=77%	RH=90%	RH=55%	RH=77%	RH=90%	RH=55%	RH=77%	RH=90%	RH=90%	RH=90%	RH=90%
30	1.03(0.08)	1.03(0.10)	1.04(0.15)	1.05(0.14)	1.07(0.17)	1.08(0.18)	1.08(0.13)	1.07(0.09)	1.09(0.13)	1.00(0.07)	1.09(0.20)	1.05(0.13)
35	1.04(0.08)	1.06(0.09)	1.08(0.13)	1.05(0.12)	1.08(0.14)	1.11(0.15)	1.08(0.11)	1.07(0.08)	1.12(0.12)	1.01(0.06)	1.11(0.16)	1.06(0.12)
41	1.04(0.06)	1.08(0.07)	1.11(0.11)	1.05(0.10)	1.09(0.12)	1.13(0.13)	1.09(0.10)	1.08(0.08)	1.14(0.10)	1.03(0.05)	1.14(0.14)	1.08(0.11)
47	1.06(0.06)	1.10(0.06)	1.16(0.09)	1.05(0.09)	1.10(0.10)	1.16(0.12)	1.09(0.09)	1.10(0.07)	1.18(0.09)	1.08(0.05)	1.17(0.13)	1.10(0.11)
55	1.07(0.05)	1.12(0.06)	1.21(0.08)	1.06(0.08)	1.12(0.09)	1.20(0.10)	1.09(0.07)	1.12(0.06)	1.22(0.08)	1.18(0.05)	1.21(0.11)	1.14(0.10)
64	1.08(0.04)	1.14(0.05)	1.25(0.07)	1.06(0.07)	1.14(0.08)	1.23(0.09)	1.11(0.06)	1.14(0.06)	1.26(0.07)	1.24(0.04)	1.25(0.10)	1.19(0.09)
75	1.09(0.04)	1.16(0.04)	1.28(0.05)	1.08(0.06)	1.15(0.07)	1.27(0.08)	1.11(0.05)	1.17(0.05)	1.30(0.06)	1.28(0.04)	1.28(0.08)	1.25(0.08)
87	1.10(0.03)	1.17(0.03)	1.31(0.04)	1.07(0.05)	1.17(0.06)	1.31(0.07)	1.11(0.04)	1.19(0.04)	1.35(0.05)	1.32(0.04)	1.31(0.07)	1.30(0.07)
101	1.10(0.03)	1.18(0.03)	1.33(0.04)	1.08(0.05)	1.18(0.05)	1.34(0.06)	1.11(0.03)	1.21(0.04)	1.37(0.04)	1.34(0.04)	1.34(0.07)	1.34(0.07)
118	1.09(0.02)	1.18(0.02)	1.33(0.03)	1.08(0.04)	1.18(0.05)	1.35(0.06)	1.11(0.03)	1.22(0.03)	1.39(0.04)	1.34(0.03)	1.35(0.06)	1.37(0.06)
137	1.09(0.02)	1.17(0.02)	1.32(0.03)	1.08(0.04)	1.18(0.04)	1.37(0.05)	1.11(0.03)	1.22(0.03)	1.40(0.03)	1.32(0.03)	1.37(0.06)	1.38(0.06)
160	1.07(0.02)	1.16(0.02)	1.30(0.03)	1.07(0.04)	1.17(0.04)	1.38(0.04)	1.10(0.03)	1.21(0.03)	1.40(0.03)	1.29(0.03)	1.38(0.05)	1.39(0.05)
186	1.06(0.02)	1.13(0.02)	1.26(0.02)	1.07(0.03)	1.18(0.03)	1.39(0.04)	1.08(0.02)	1.20(0.02)	1.39(0.03)	1.25(0.03)	1.41(0.04)	1.39(0.05)
217	1.05(0.02)	1.12(0.02)	1.22(0.02)	1.06(0.03)	1.17(0.03)	1.39(0.03)	1.07(0.02)	1.18(0.02)	1.37(0.03)	1.22(0.02)	1.42(0.04)	1.40(0.04)
252	1.05(0.02)	1.11(0.02)	1.19(0.02)	1.06(0.02)	1.17(0.02)	1.40(0.03)	1.06(0.02)	1.17(0.02)	1.35(0.02)	1.19(0.02)	1.43(0.03)	1.41(0.04)
294	1.05(0.02)	1.11(0.02)	1.17(0.02)	1.06(0.02)	1.17(0.02)	1.40(0.02)	1.05(0.02)	1.17(0.02)	1.33(0.02)	1.17(0.02)	1.43(0.02)	1.42(0.03)
342	1.05(0.02)	1.11(0.02)	1.15(0.01)	1.06(0.02)	1.16(0.02)	1.39(0.01)	1.05(0.02)	1.16(0.02)	1.32(0.02)	1.18(0.02)	1.42(0.02)	1.48(0.02)
398	1.04(0.01)	1.08(0.01)	1.14(0.01)	1.05(0.01)	1.15(0.01)	1.37(0.02)	1.05(0.02)	1.15(0.02)	1.31(0.02)	1.19(0.02)	1.40(0.01)	1.42(0.02)

Title Page

Abstract

Introduction

Conclusions

References

Tables

Figures

◀

▶

◀

▶

Back

Close

Full Screen / Esc

Printer-friendly Version

Interactive Discussion



Hygroscopic growth of urban aerosol particles in Beijing

J. Meier et al.

Table A3. Hygroscopic descriptive growth factors, calculated on the basis of H-TDMA measurements for the three different air masses (A1, A2, A3) at a relative humidity of 90%.

D_p [nm]	A1 (17-01-2005 12:00 –20-01-2005 19:00)	A2 (20-01-2005 19:00 –24-01-2005 01:00)	A3 (24-01-2005 01:00 –25-01-2005 10:00)
30	1.10(0.01)	1.12(0.01)	1.13(0.02)
50	1.29(0.03)	1.30(0.03)	1.31(0.04)
80	1.39(0.05)	1.41(0.05)	1.44(0.05)
150	1.34(0.04)	1.43(0.04)	1.42(0.04)
250	1.25(0.04)	1.41(0.05)	1.35(0.05)
350	1.21(0.03)	1.37(0.05)	1.33(0.04)

Title Page

Abstract

Introduction

Conclusions

References

Tables

Figures

◀

▶

◀

▶

Back

Close

Full Screen / Esc

Printer-friendly Version

Interactive Discussion



Hygroscopic growth of urban aerosol particles in Beijing

J. Meier et al.

Table A4. Hygroscopic descriptive growth factors, calculated by a model based on the particles collected with MOUDI (I1, I2, I3) at a relative humidity of 90%.

Time Period	D_p [nm]	Run 1	Run 2	Run 3	Run 4	Run 5	Run 6
I1 (17-01-2005 12:00 –18-01-2005 12:00)	75	1.28(0.14)	1.38(0.18)	1.28(0.14)	1.28(0.14)	1.38(0.18)	1.38(0.18)
	135	1.32(0.16)	1.41(0.19)	1.32(0.16)	1.32(0.16)	1.41(0.19)	1.41(0.19)
	240	1.31(0.15)	1.31(0.15)	1.30(0.14)	1.26(0.13)	1.31(0.15)	1.38(0.17)
	420	1.29(0.13)	1.19(0.09)	1.17(0.08)	1.14(0.07)	1.30(0.13)	1.35(0.15)
I2 (22-01-2005 14:00 –23-01-2005 14:00)	760	1.19(0.08)	1.11(0.05)	1.09(0.04)	1.05(0.03)	1.21(0.09)	1.26(0.11)
	42	1.22(0.11)	1.22(0.11)	1.22(0.11)	1.22(0.11)	1.22(0.11)	1.22(0.11)
	75	1.28(0.13)	1.35(0.16)	1.28(0.13)	1.28(0.13)	1.35(0.16)	1.35(0.16)
	135	1.32(0.15)	1.40(0.18)	1.32(0.15)	1.32(0.15)	1.40(0.18)	1.40(0.18)
	240	1.34(0.16)	1.39(0.18)	1.34(0.16)	1.34(0.16)	1.39(0.18)	1.39(0.18)
I3 (23-01-2005 16:00 –24-01-2005 12:00)	420	1.30(0.14)	1.35(0.16)	1.30(0.14)	1.30(0.14)	1.35(0.16)	1.35(0.16)
	760	1.22(0.10)	1.22(0.10)	1.21(0.10)	1.19(0.09)	1.22(0.10)	1.26(0.12)
	75	1.36(0.17)	1.42(0.19)	1.36(0.17)	1.36(0.17)	1.42(0.19)	1.42(0.19)
	135	1.35(0.17)	1.42(0.19)	1.35(0.17)	1.35(0.17)	1.42(0.19)	1.42(0.19)
	240	1.39(0.18)	1.43(0.19)	1.39(0.18)	1.39(0.18)	1.43(0.19)	1.43(0.19)
	420	1.38(0.18)	1.41(0.19)	1.38(0.18)	1.38(0.18)	1.41(0.19)	1.41(0.19)
	760	1.29(0.13)	1.24(0.11)	1.24(0.11)	1.22(0.11)	1.24(0.11)	1.33(0.15)

Title Page

Abstract

Introduction

Conclusions

References

Tables

Figures

◀

▶

◀

▶

Back

Close

Full Screen / Esc

Printer-friendly Version

Interactive Discussion



Hygroscopic growth
of urban aerosol
particles in Beijing

J. Meier et al.

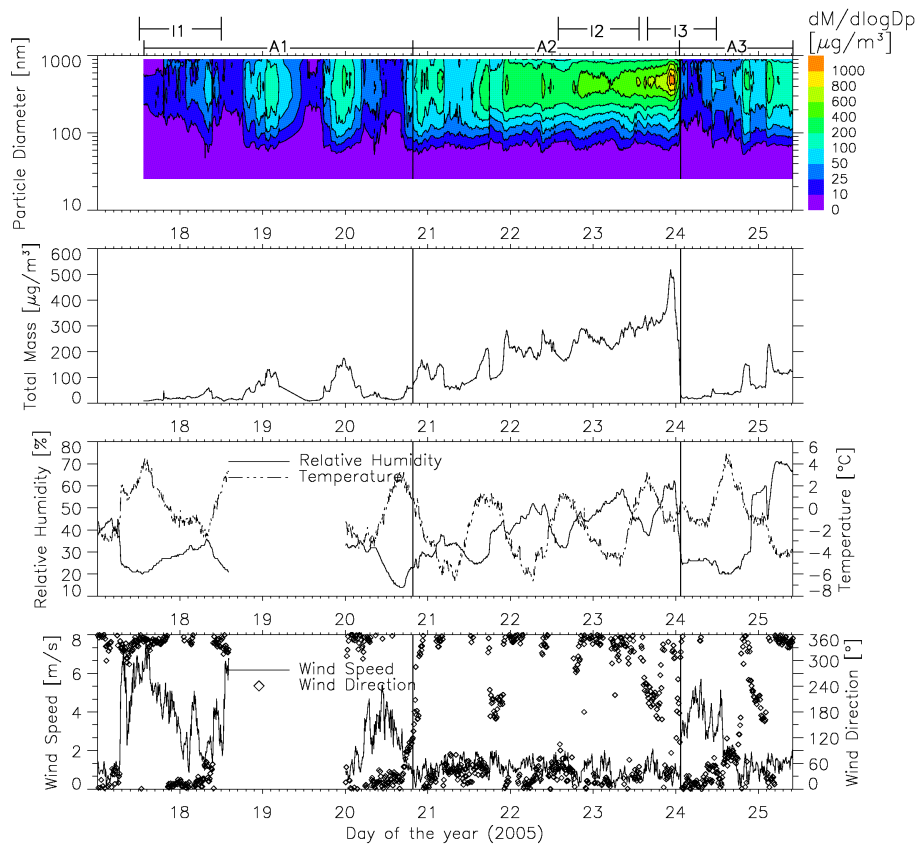


Fig. 1. Particle mass size distribution, temperature, relative humidity, wind speed and wind direction during the measurement campaign in Beijing from 17 to 25 January 2005.

[Title Page](#)[Abstract](#)[Introduction](#)[Conclusions](#)[References](#)[Tables](#)[Figures](#)[◀](#)[▶](#)[◀](#)[▶](#)[Back](#)[Close](#)[Full Screen / Esc](#)[Printer-friendly Version](#)[Interactive Discussion](#)

Hygroscopic growth of urban aerosol particles in Beijing

J. Meier et al.

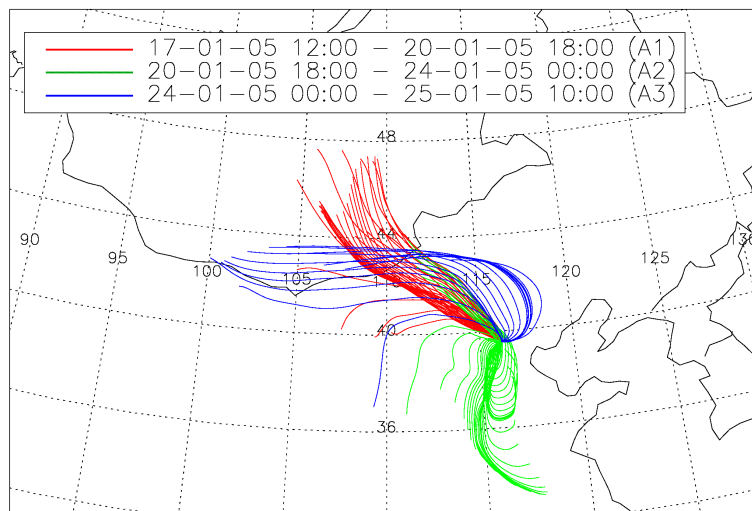


Fig. 2. Back trajectories in Beijing (air mass A1, red), 20-01-05 19:00 and 24-01-05 01:00 (air mass A2, green), 24-01-05 01:00 and 25-01-05 10:00 (air mass A3, blue). Trajectory length was 48 h. Trajectories were started every three hour. Source: HYSPLIT website (Draxler and Hess, 2004).

Title Page

Abstract

Introduction

Conclusions

References

Tables

Figures

◀

▶

◀

▶

Back

Close

Full Screen / Esc

Printer-friendly Version

Interactive Discussion



Hygroscopic growth
of urban aerosol
particles in Beijing

J. Meier et al.

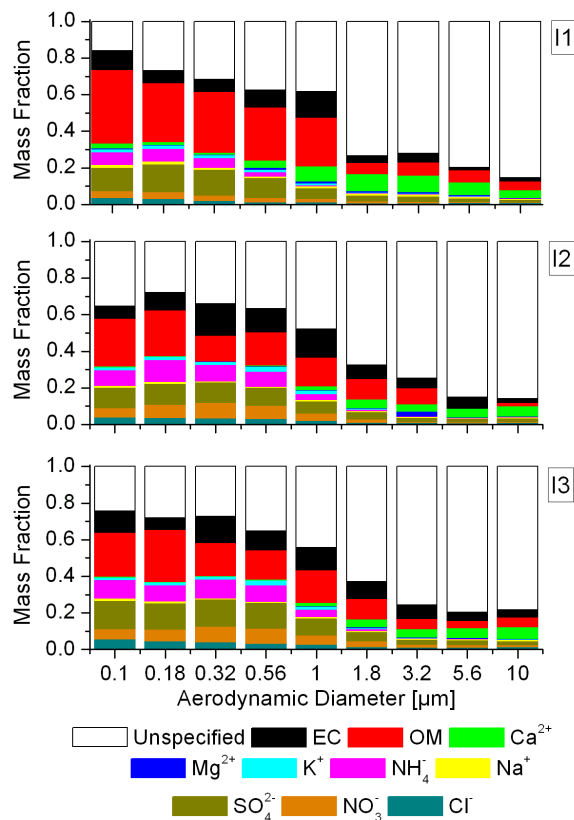


Fig. 3. Mass fractions of inorganic ions, EC, OM and the unspecified remainder within ten aerodynamic size classes during the three measurement periods 17-01-2005 to 18-01-2005 (I1, top), 22-01-2005 to 23-01-2005 (I2, middle) and 23-01-2005 to 24-01-2005 (I3, bottom). The unspecified material is assumed to consist of insoluble material.

[Title Page](#)[Abstract](#)[Introduction](#)[Conclusions](#)[References](#)[Tables](#)[Figures](#)[◀](#)[▶](#)[◀](#)[▶](#)[Back](#)[Close](#)[Full Screen / Esc](#)[Printer-friendly Version](#)[Interactive Discussion](#)

Hygroscopic growth of urban aerosol particles in Beijing

J. Meier et al.

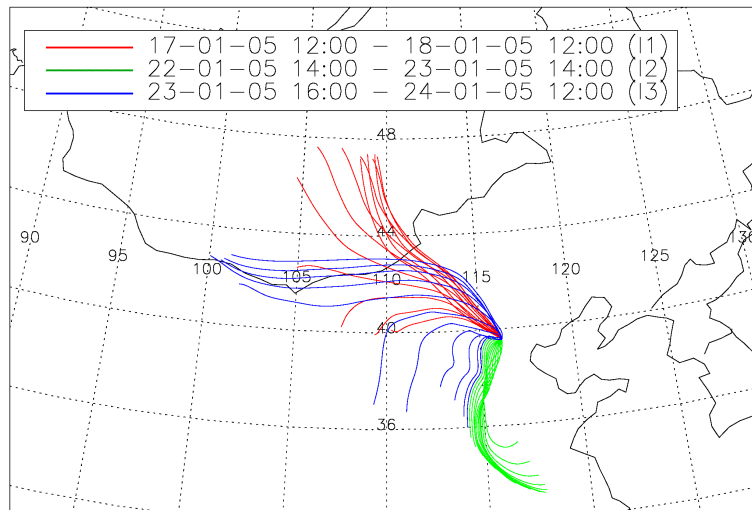


Fig. 4. Back trajectories arriving at Beijing during the impactor sampling periods I1 (red), I2 (green) and I3 (blue). Trajectory length is 48 h. Each trajectory represents a three hour interval. Source: HYSPLIT website (Draxler and Hess, 2004).

Title Page

Abstract

Introduction

Conclusions

References

Tables

Figures

◀

▶

◀

▶

Back

Close

Full Screen / Esc

Printer-friendly Version

Interactive Discussion



Hygroscopic growth
of urban aerosol
particles in Beijing

J. Meier et al.

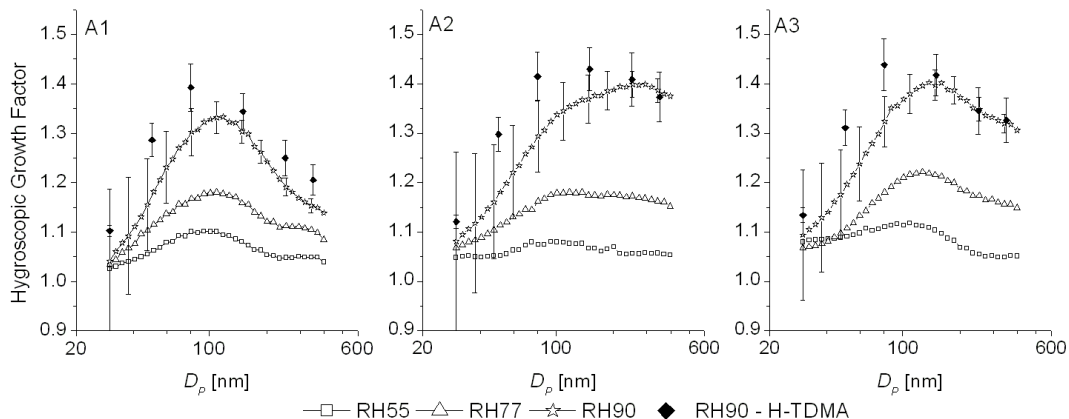


Fig. 5. Descriptive hygroscopic growth factors as a function of particle size for the three investigated air masses (A1, A2, A3). Data derived from the H-DMPS/TDMPS are shown for three selected relative humidities (RH=55%, 77% and 90%), complemented by individual data points obtained by the H-TDMA at six particle diameters (30 nm, 50 nm, 80 nm, 150 nm, 250 nm, 350 nm) and 90% relative humidity. The error bars indicate the measurement errors.

[Title Page](#)[Abstract](#)[Introduction](#)[Conclusions](#)[References](#)[Tables](#)[Figures](#)[◀](#)[▶](#)[◀](#)[▶](#)[Back](#)[Close](#)[Full Screen / Esc](#)[Printer-friendly Version](#)[Interactive Discussion](#)

Hygroscopic growth
of urban aerosol
particles in Beijing

J. Meier et al.

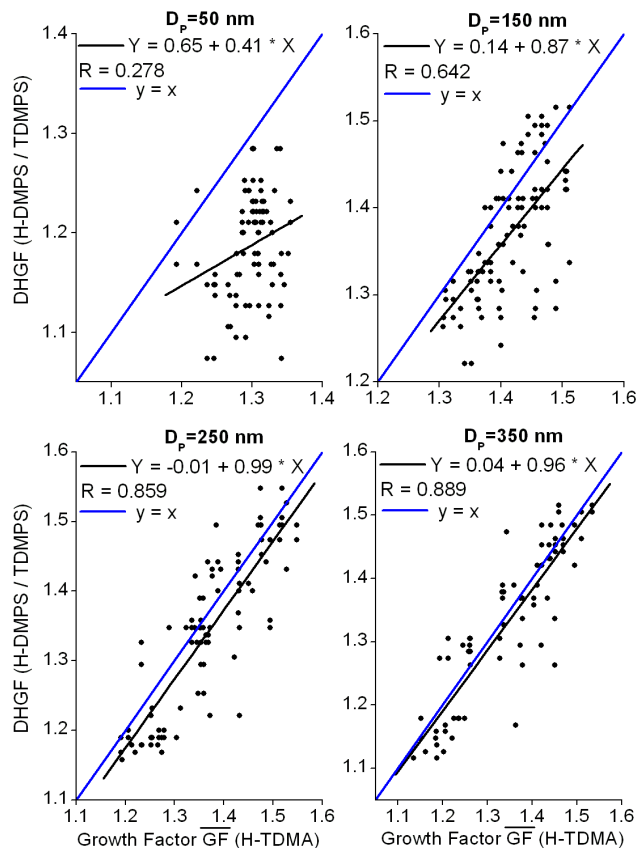


Fig. 6. Correlation coefficients for $D_p=50$ nm (top left), $D_p=150$ nm (top right), $D_p=250$ nm (down left) and $D_p=350$ nm (down right) between the DHGF (H-DMPS/TDMPS) and the \overline{GF} (H-TDMA).

[Title Page](#)[Abstract](#)[Introduction](#)[Conclusions](#)[References](#)[Tables](#)[Figures](#)[◀](#)[▶](#)[◀](#)[▶](#)[Back](#)[Close](#)[Full Screen / Esc](#)[Printer-friendly Version](#)[Interactive Discussion](#)

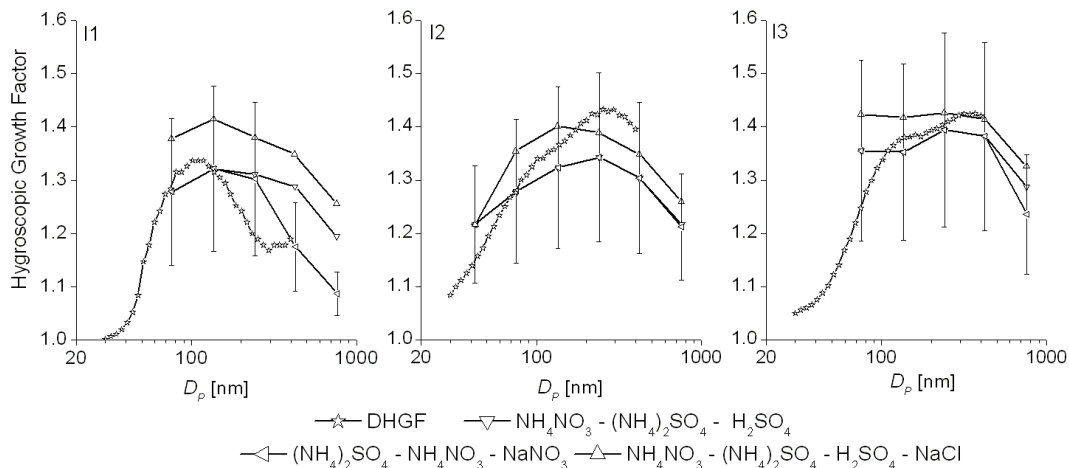


Fig. 7. Descriptive hygroscopic growth factor distributions DHGF based on TDMPs and H-DMPs measurements and three runs of the calculated hygroscopic growth factors CHGF calculated at RH=90% based on MOUDI samples during the three measurement periods (I1, I2, I3).

Hygroscopic growth of urban aerosol particles in Beijing

J. Meier et al.

Title Page

Abstract

Introduction

Conclusions

References

Tables

Figures

◀

▶

◀

▶

Back

Close

Full Screen / Esc

Printer-friendly Version

Interactive Discussion

